



## **PROBABILISTIC ASSESSMENT OF OFFSHORE PIPELINE UNDER CORROSION DEFECTS**

**Wokocha Heanyichukwu, \*Nitonye Samson, Sidum Adumene and Morrison Inegiyemiema**

*Department of Marine Engineering, Rivers State University, Port-Harcourt, Nigeria.*

**\*Corresponding Author:** [nitonye.samson@ust.edu.ng](mailto:nitonye.samson@ust.edu.ng)

**Keywords:** Pipeline, Corrosion, Defects, Integrity, Risk, Assessment, Failure

**Abstract:** The current study provides a detailed analysis of corrosion behaviour and integrity management strategies for offshore pipelines, addressing key challenges in subsea environments. Integrated empirical and probabilistic methods were adopted to evaluate corrosion mechanisms, considering defect profiling, stress analysis, and risk assessment. The study shows that at the initiation of corrosion, the pipeline thickness results in strength with time. Further analysis revealed that corrosion rates rise significantly with water temperatures above 15°C but progress more slowly below this threshold, supporting predictive models and corroborated by literature. While defect length increases steadily, the depth reaches a plateau after around 20 years, underscoring the need for continuous monitoring to manage defect progression effectively. A strong correlation was found between increased corrosion defect length and decreased failure stress ratio. For instance, after 25 years without protection, the pipeline can handle only 20% of its original design stress, reducing structural capacity. The probability of failure grows over time as the failure stress ratio drops. For example, after 17 years, with a failure stress ratio of 45%, the failure probability is 51%, rising to 75% by 25 years without protection. A comprehensive framework is proposed, integrating probabilistic risk assessment, stress load evaluation, and targeted corrosion mitigation strategies to enhance pipeline safety and reliability through structured maintenance and proactive management.

### **1. Introduction**

Offshore pipelines are essential in the oil and gas industry for transporting hydrocarbons from offshore production facilities to onshore processing plants. However, they face significant challenges due to corrosion caused by environmental factors such as seawater exposure, fluctuating temperatures, and marine organisms. Corrosion can lead to serious integrity issues, including leaks and operational

disruptions, making effective corrosion management critical. This management relies on routine inspections, protective coatings, and cathodic protection, as well as a thorough understanding of corrosion processes and the material properties of the pipelines. Recent advancements in corrosion monitoring technologies and predictive models using machine learning have enhanced the ability to manage pipeline integrity effectively.

**Wokocha Heanyichukwu, Nitonye Samson, Sidum Adumene and Morrison Inegiyemiema**



Nevertheless, challenges remain due to the unpredictable marine environment and limitations in data acquisition.

The current study presents a probabilistic analysis of offshore pipelines under corrosion defects. The analysis focuses on corrosion depth profiles under the different empirical models to determine the likely failure characteristic of the pipeline. Key considerations were given to evaluating corrosion influencing factors, exploring empirical models for predicting corrosion depth, and assessing mitigation techniques. The significance of the research lies in improving understanding of corrosion mechanisms, optimizing management strategies, and advancing predictive models for better decision-making. The research outcome provides technical information that would enhance risk-based integrity management of the asset.

## 2. Materials and Methods

This chapter presents a mixed-methods methodology for studying and managing offshore pipeline corrosion, integrating quantitative and qualitative approaches. The research process consists of four phases: data collection, data analysis, model development, and framework formulation, ensuring a logical progression of research efforts (Johnson & Smith, 2018).

Key factors influencing CO<sub>2</sub>-driven corrosion in carbon-steel oil pipelines include temperature, partial CO<sub>2</sub> pressure, fluid flow regime, liquid velocity, pH value, and concentration of corrosion products (FeCO<sub>3</sub>). By investigating these variables, the study aims to develop predictive models for corrosion behavior. The pipeline material is carbon steel ASTM A36 grade, with a Young's Modulus of 200 GPa, yield stress of 250 MPa, and ultimate tensile stress ranging from 400 to 550 MPa, as detailed in Table 1.

**Table 1: Subsea Transmission Pipeline Characteristics**

Particulars	Parameters
Pipe size	254 mm (10")
Pipe length	3500 m (12 m is used for the analysis)
Nominal wall thickness	18 mm
Internal diameter	236 mm
Outer diameter	272 mm
Pipe inlet pressure	34.4 bar
Pipe inlet temperature	89°C - 95°C
Operation time	6 years
Pipe roughness	0.04572 mm
Wall shear stress	0.57 - 8.57 Pa
Standard used	BS31.3
Seawater temperature	5°C, 15°C and 95°C
Seawater average PH	6.0
Fluid type	Multiphase
Partial pressure of CO <sub>2</sub>	5.92 - 7.28 bar
Gas velocity	0.20 - 0.24 m/s
Liquid velocity	0.44 - 2.13 m/s

**Wokocha Heanyichukwu, Nitonye Samson, Sidum Adumene and Morrison Inegiyemiema**



## 2.1 Data Collection Methods

This study uses a two-pronged approach to investigate corrosion factors. First, modern corrosion monitoring devices are installed on active offshore pipelines to collect real-time data on corrosion rates and environmental factors like temperature, humidity, salinity, flow rate, and pressure. Pipeline material properties are also recorded to analyze their impact on corrosion. Simultaneously, a literature review explores established research on corrosion causes and mitigation strategies, combining empirical data with existing knowledge to strengthen future studies (Williams & Brown, 2019).

### 2.1.1 Mechanism of Corrosion

Corrosion in steel occurs when exposed to corrosive environments, such as seawater, leading to electrochemical reactions where metal atoms lose electrons ( $M \rightarrow M^{n+}$ ) (Bai & Bai, 2014; Nitonye et al., 2020).

The anode usage factor reflects the effectiveness of anodes in providing cathodic protection and exceeding this factor can impair performance. Offshore anodes are typically made from zinc or aluminum, with aluminum preferred for its electrochemical capabilities, while zinc is often more reliable in specific conditions (DNV 1993; DNV 2010). Understanding metal electrochemical activity and the Galvanic Series is essential for effective corrosion management, as detailed in Table 2

**Table 2: Design Utilization Factors for Different Types of Anodes**

Anode Type	Anode Utilization Factor
Long 1) slender stand-off	0.90
Long 1) flush-mounted	0.85
Short 2) flush-mounted	0.80
Bracelet, half-shell type	0.80
Bracelet, segmented type	0.75

### 2.1.2. Prediction of Corrosion Rate and Wear of Carbon Steel

The corrosion model illustrates the corrosion and wear rate (Qin & Cui 2003; Nitonye et al 2018). The use of this model and its modifications to predict corrosion in both general and specific conditions is common.

Equations (1) and (2) show how rusting occurs.

$$C_r(t) = d_{\infty} \frac{\beta}{\eta} \left( \frac{t-T_{St}}{\eta} \right)^{\beta-1} \cdot \exp \left\{ - \left( \frac{t-T_{St}}{\eta} \right)^{\beta} \right\} \quad (1)$$

$$C_w(t) = d_{\infty} \left\{ 1 - \exp \left[ - \left( \frac{t-T_{St}}{\eta} \right)^{\beta} \right] \right\} \quad (2)$$

Where: time is  $0 \leq t \leq T_{St}$  and  $T_{St} \leq t \leq T_L$

$C_r(t)$  = Corrosion rate at time “t”,

$C_w(t)$  = Corrosion wear at time “t”,

**Wokocha Heanyichukwu, Nitonye Samson, Sidum Adumene and Morrison Inegiyemiema**



$d_{\infty}$  = Long-term corrosion wastage of pipe thickness

$$d_{\infty} = d_{\max} + D_d$$

$T_{St}$  = Instant at which corrosion is observed,

$T_L$  = Life of the structure,

$d_{\max}$  = the maximum wear in the distribution

$D_d$  = chosen as  $d_{\max}$  100.

## 2.2 Empirical Model Evaluation

Evaluating empirical models for predicting corrosion depth requires a structured assessment strategy. This study selects various corrosion prediction models based on a thorough literature review and the collected field data. The models include machine learning algorithms, mechanistic models, and statistical regression techniques.

Each selected model generates anticipated corrosion depths based on historical corrosion data and current environmental conditions. The accuracy and reliability of these models are rigorously assessed by comparing predictions to actual corrosion data. Key performance metrics, such as mean squared error and correlation coefficients, are employed to evaluate each model's effectiveness. This comprehensive evaluation aims to provide reliable tools for estimating corrosion depths across diverse operational contexts, ultimately leading to the development of models with enhanced predictive capabilities (Johnson & Smith 2018).

However, Equation (1) can be rewritten as:

$$-In\left(-In\left(1 - \frac{d(t)}{d_{\infty}}\right)\right) = \beta In\eta - \beta In(t - T_{St}) \quad (3)$$

$$If \begin{cases} Y = -In\left(-In\left(1 - \frac{d(t)}{d_{\infty}}\right)\right) \\ X = In(t - T_{St}) \\ A = \beta In\eta \\ B = -\beta \\ \eta = \exp(A\beta) \end{cases}$$

Then, Equation (2) reduces to:

$$Y = A + BX \quad (4)$$

$\beta$ ,  $\eta$ ,  $d_{\infty}$  and  $T_{St}$  are the four random parameters of the model corresponding to (Johnson & Smith 2018).

$$d_{\infty} = 1.8281$$

$$T_{St} = 1.40, \beta = 0.3915$$

$$\eta = 1.5180$$

Applying equation (3) using these values and by linear regression produces the line with:

$$A = 0.1634 \text{ and } B = -0.3915.$$

Thus, the line is:

$$Y = 0.1634 - 0.3915X \quad (5)$$

From Equation (5), the random parameters for Equations (3) and (4) can be derived as:

$$\beta = -B = 0.3915 \text{ and}$$

$$\eta = \exp\left(\frac{A}{\beta}\right) = \exp\left(\frac{0.1634}{0.3915}\right) = 1.5180$$

For this analysis, the effect of flow on sweet corrosion rate can be estimated using a resistance model as:

$$U_{cr} \frac{1}{\frac{1}{U_r} + \frac{1}{U_m}} \quad (6)$$

Where:

$U_{cr}$  = the corrosion rate in mm/year,

$U_r$  = the flow-independent reaction rate,

**Wokocha Heanyichukwu, Nitonye Samson, Sidum Adumene and Morrison Inegiemiema**



$U_m$  = the flow-dependent mass transfer rate.

For a multiphase turbulent flow in a pipeline,

$U_m$  = dependent on the flow velocity and the liquid film thickness.

It can be estimated as:

$$U_m = 2.45 \cdot \frac{U^{0.8}}{d^{0.2}} \cdot pCO_2 \quad (7)$$

Where the partial pressure of  $CO_2$  in bar, symbolized by  $pCO_2$  can be obtained using the relationship:

$$pCO_2 \begin{cases} \frac{M_{CO_2}(kmole/h)}{M_T \text{ flow}(kmole/h)} \times P \\ \frac{\text{mole\% } CO_2(g)}{100} \times P \end{cases} \quad (8)$$

## 2.2.1. Temperature and pH Dependencies of Corrosion Rate

The corrosion rate ( $CR_t$ ) in  $mm/year$  can be estimated more accurately by a set of temperature and pH-dependent models, which are expressed as follows:

For  $20^\circ C \leq T \leq 150^\circ C$ :

$$CR_t = K_t \times fCO_2 \times fp_H \times \left(\frac{S}{19}\right)^{0.146 + 0.0324 \log(fCO_2)} \quad (9)$$

For  $T = 15^\circ C$ :

$$CR_t = 0.36K_t \times fCO_2 \times fp_H \times \left(\frac{S}{19}\right)^{0.146 + 0.0324 \log(fCO_2)} \quad (10)$$

For  $T = 5^\circ C$ :

$$CR_t = 0.36K_t \times fCO_2 \times fp_H \quad (11)$$

The kinetics of corrosion are influenced by temperature, and surface temperature is a key element. The corrosion rate will significantly

accelerate when the surface temperature rises to the point at which the electrolyte evaporates. According to (Guedes *et al.* 2011) and Pohlman (1987), the corrosion rate will significantly reduce at this temperature. By using linear interpolation, it is possible to determine the corrosion rate between temperatures.

Table 2. provides the associated corrosion constant  $K_t$  and pH function. Gases are not ideal at high pressure, and a fugacity constant can be used to adjust the partial pressures of such gases. The following formula represents the fugacity function of  $CO_2$  pressure:

$$fCO_2 = a \times p \quad (12)$$

The fugacity coefficient is given as

$$a \begin{cases} 10^{p \times (0.0031 - 1.4/T)} \rightarrow \text{for } P \leq 250 \text{ bar} \\ 10^{p \times (0.0031 - 1.4/T)} \rightarrow \text{or } P \geq 250 \text{ bar} \end{cases} \quad (13)$$

Temperatures  $T = 5^\circ C$ ,  $T = 15^\circ C$ , and  $T = 20^\circ C$  are put into practice because water depths of less than 500 m and an average pH of 6.0 are considered.

The following equations are used to compute the pH and fugacity functions for the selected temperatures:

## 2.2.2. The Remaining Strength Criteria of Corroded Pipeline

It is essential to assess the pipe's residual strength to determine the corroded pipe's integrity. The permissible maximum length of flaws, permissible maximum pressure for uncoded pipes, and maximum safe pressure are some evaluation criteria for corroded pipelines.





Equation (19) is used to approximate the projected hoop stress level upon failure of corroded pipe based on these:

$$S_F = S_{flow} \left( \frac{1 - A_R}{1 - A_R/M_F} \right) \quad (14)$$

Where:

$S_{flow}$  = the flow stress of the material,

$A_R$  = the area ratio

$$A_R = \frac{A_{flaw}}{A_0}$$

$A_{flaw}$  = the area of through-thickness profile of flaw

$A_0$  = the area of uncorroded equivalence to flaw profile

$$A_0 = L \times t$$

Similarly:

$L$  = the maximum axial range of the defect,

$T$  = the nominal wall thickness of the pipe,

$D$  = the nominal diameter of the pipe

$M_F$  = the Folias factor, which is determined by:

$$M_F = \sqrt{1 + \frac{0.8 \times L^2}{D \times t}} \quad (15)$$

## 2.2.3. Allowable Maximum Length and Depth of Defect

The maximum allowable corroded length for a defect depth “ $d$ ”, nominal wall thickness “ $t$ ”, nominal diameter “ $D$ ”, and depth ratio ( $d_R$  =

## 3. RESULTS AND DISCUSSION:

### 3.1. Reduction in pipeline thickness over time

Figure 1 depicts the phenomenon of pipeline thickness reduction over time due to corrosion, using Equations (6) and (7).

$d/t$ ) in the range of  $0.1 < d_R < 0.8$ , is estimated using Equation (16):

$$LD = 1.12 \sqrt{D \times t \left[ \left( \frac{dR}{1.1dR - 0.15} \right)^2 - 1 \right]} \quad (16)$$

By equating the maximum allowable operating pressure to the maximum allowable design pressure, the maximum allowable defect depth can be estimated as

When  $A \leq 4$

$$d_{max} = 1.5t \left[ \frac{1 - k}{1 - k\sqrt{A^2 + 1}} \right] \quad (17)$$

When  $A > 4$   $d_{max} = t(1 - k)$  Where: the pressure ratio,

$$k = pop. \frac{max}{1.1p_{max}} \text{ and } A = 0.803 \frac{L}{\sqrt{D \times t}}$$

However, when the safe maximum pressure is  $P_{safe} < P_{max}$  and  $A \leq 4$ , its value is given by Equation (13)

### 2.3 Data Analysis

In this study, the application of empirical and mechanistic models, such as the Qin and Cui model, plays a crucial role in deriving corrosion depth profiles and pipeline failure predictions. Equations (1) and (2) are applied to estimate the corrosion rate over time and to determine the expected pipeline thickness reduction. Using empirical data, these models generate the results shown in section 3.

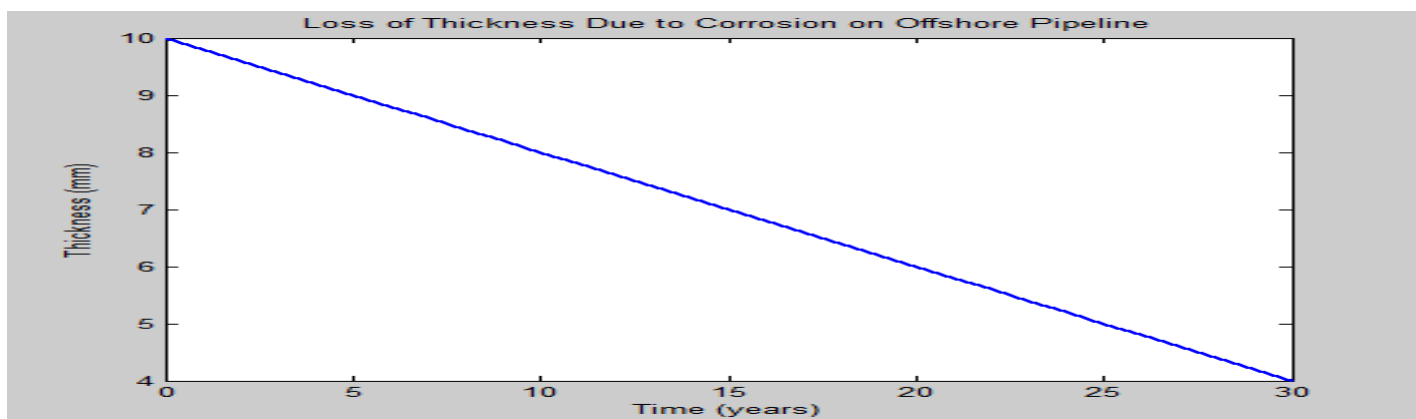


**Fig. 1: Loss of Thickness Due to Corrosion on Offshore Pipeline**

Figure 1 describes the concentration of rust and wear over time, which directly affect the thickness reduction. The result shows a gradual decrease in pipeline thickness, aligning with predictions made by researchers such as Qin and Cui (2003). Despite using corrosion inhibitors, no subsea pipeline is entirely immune to corrosion. Initially rapid, corrosion slows over time; the data analysis reveals a decline in thickness reduction rate as the pipeline ages, aligning with existing literature. This aging process signifies corrosion becoming less aggressive over time, which is crucial for maintenance decisions.

### 3.2. How corrosion rate is affected by temperature

Figure 2 depicts the relationship between corrosion rate and water temperature, elucidated by Equations (11) and (12).

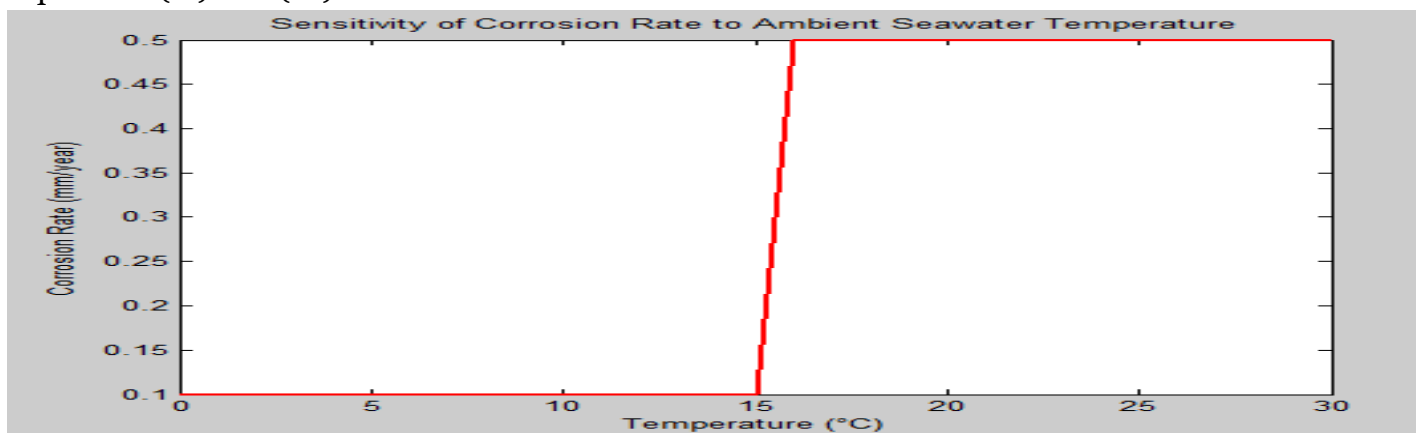


**Fig. 2: Sensitivity of Corrosion Rate to Ambient Seawater Temperature**

**Wokocha Heanyichukwu, Nitonye Samson, Sidum Adumene and Morrison Inegiyemiema**



The result in Figure 2 revealed the intricate interplay between corrosion rate and water temperature. Corrosion progresses more slowly at temperatures below 15°C, as evidenced by the gradual curve in the figure. Conversely, temperatures exceeding 15°C accelerate corrosion rates, resulting in a steeper curve. This observed relationship aligns with the predictive model proposed by Qin and Cui (2011), as substantiated by Guedes *et al.* (2011), emphasizing the pivotal role of temperature in shaping corrosion dynamics. Understanding these temperature-corrosion rate dynamics is imperative for proactive corrosion management in offshore pipelines, particularly in shallow waters characterized by higher temperatures.

A comparative analysis with existing literature, particularly studies by Guedes *et al.* (2011), corroborates the observed trend of faster corrosion rates in warmer water environments. This alignment enhances the credibility of this analysis and underscores the significance of temperature in corrosion dynamics.

### 3.3. Corrosion Depth Profiling using Empirical and Exponential Models

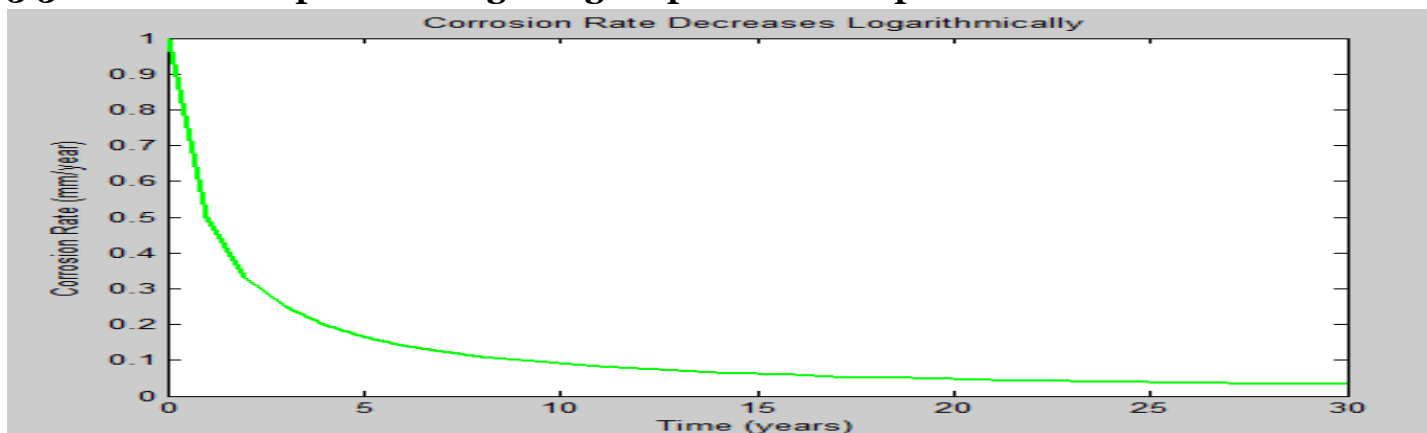


**Fig. 3a. Corrosion Rate (Empirical Model)**

Figure 3 shows the analysis employed using empirical models for corrosion depth profiling. The analysis describes the concentration of rust and wear over time, contributing to corrosion depth. By comparing the findings with empirical data and research models, such as those presented by Bia and Youde (2019), there is a logarithmic decrease in corrosion rate over time. This confirmation reinforces my empirical modelling approach's credibility and applicability to real-world scenarios. The result of the exponential model is shown in Figure 3b.



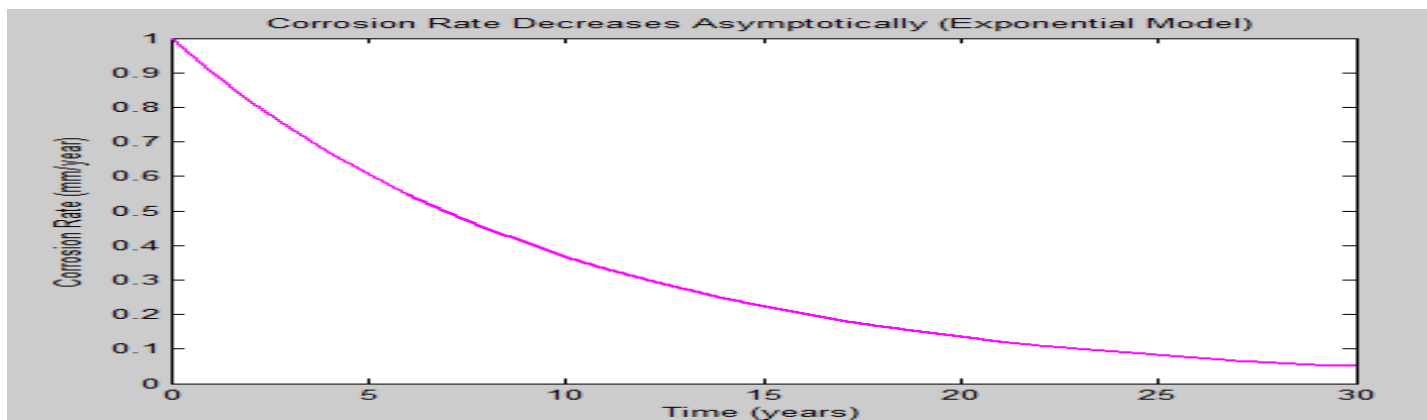


**Fig. 3b: Corrosion Rate (Exponential Model).**

The result shows a logarithmic decrease in corrosion rate over time, attributed to the formation of protective layers of corroded metal oxides on the pipe's surface. These layers act as a shield, mitigating the impact of harmful elements and impeding further corrosion. The concept of corrosion rate attenuation aligns with findings from the study by Bia and Youde (2019), which emphasizes the significance of these protective layers in early detection and prevention of pipeline failures. Understanding this logarithmic decline in corrosion rate provides valuable insights for predicting and managing corrosion in offshore pipelines, contributing to proactive maintenance strategies.

### 3.4. Corrosion Defect Length Ratio and Depth Ratio

Figure 4 shows variations in corrosion defect length ratio and depth ratio over time.

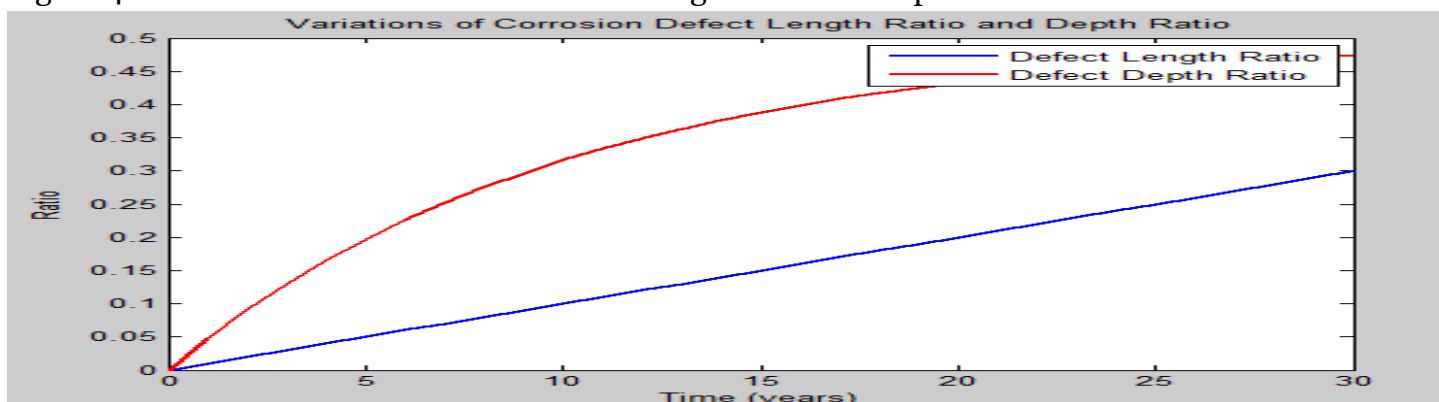


**Fig. 3.4: Variations of Corrosion Defect Length Ratio and Depth Ratio for Service Pipelines**



As the corrosion in subsea pipelines evolves continuously over time, the length of the corrosion defect steadily increases, while the corrosion depth reaches a plateau after approximately 20 years of use. This observation highlights a critical aspect of corrosion dynamics, where the defect length continues to expand while the depth stabilizes over time. Such insights underscore the importance of proactive maintenance strategies to mitigate the progression of corrosion and ensure the integrity of subsea pipelines over their operational lifespan. By comparing the results with existing literature and empirical data, the trend was observed, and the effectiveness of the analytical approach was shown in predicting corrosion behaviour in subsea pipelines.

### 3.5 Ratios of Stress Leading to Pipeline Failure and Corrosion Length

Examining the relationship between the failure stress ratio and corrosion defect length ratio describes the projected hoop stress level and the Folias factor.

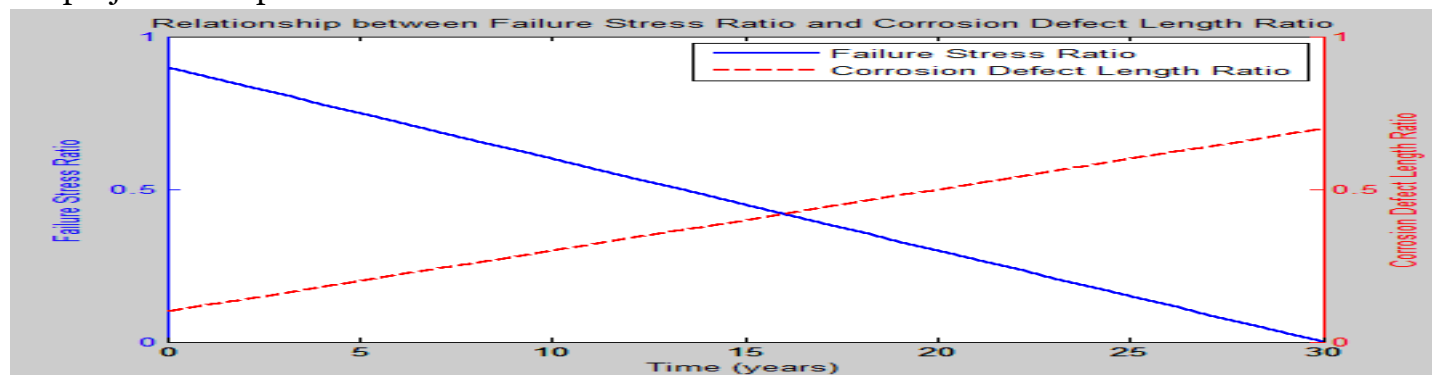


**Fig. 5: Relationship between Failure Stress Ratio and Corrosion Defect Length Ratio of a Subsea Hydrocarbon Pipeline under Service Loads**

In Figure 5, the failure stress ratio was plotted alongside the corrosion defect length ratio over time. The analysis revealed a clear correlation: as the corrosion defect in the system increased in length, the failure stress ratio decreased. This observation indicates that the system's ability to withstand stress diminishes as corrosion progresses. For example, when the pipeline has been used for 2 to 5 years and there is no significant corrosion because the coating is intact, it can handle stress up to 90% of its design limit. But after 25 years, if we do nothing to prevent corrosion, it can only handle about 20% of the design stress limit. So, it could break under much lower stress than it is designed for. To prevent this, we take steps to protect subsea pipelines from corrosion.

Based on the analysis, the likely stress level that could cause the pipeline to break under corrosion is approximately 20% of its original design stress limit. For example, If a pipeline is designed with a stress limit of 10 MPa (Mega Pascal), and after 25 years without corrosion protection, the failure stress ratio

**Wokocha Heanyichukwu, Nitonye Samson, Sidum Adumene and Morrison Inegiyemiema**



falls to 20%, then the pipeline would be at risk of breaking under a stress level as low as  $(10 \text{ MPa} \times 0.2) = 2 \text{ MPa}$ .

The correlation between corrosion defect length and pipeline reliability was confirmed by comparing the findings with established failure criteria and stress analysis models. This confirmation highlights the importance of considering corrosion effects in assessing pipeline integrity and reinforces the necessity of corrosion protection measures.

### 3.6. Probability of Pipeline Failure and Stress Comparison

The assessment of the probability of pipeline failure is informed by the principles discussed in Chapter 3, particularly Equation (3.18) and (3.19), which describe the relationship between failure stress ratio and maximum allowable defect depth.

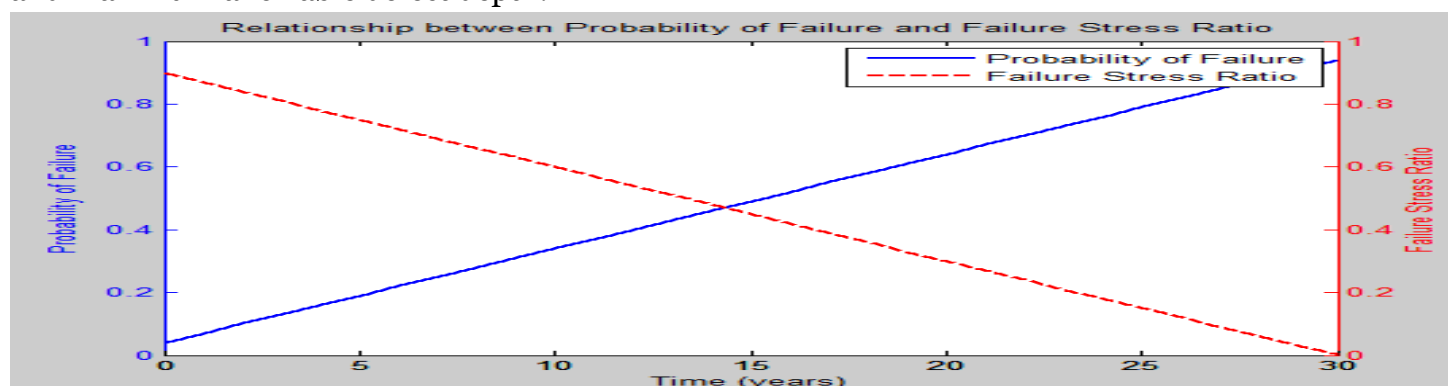


**Fig. 6: Relationship between the probability of failure and failure stress ratio of a subsea hydrocarbon pipeline**

The probability of pipeline failure is assessed using the "failure stress ratio" and the "probability of failure," as depicted in Figure 6. A high failure stress ratio, such as 90%, corresponds to a low probability of pipeline failure, around 4%, indicating reliability. However, as the failure stress ratio decreases, the probability of failure increases. For instance, after 17 years, with a failure stress ratio of 45%, the probability of failure rises to 51%, signaling increased risk. By 25 years, without protection, the failure stress ratio drops further to 20%, and

the probability of failure escalates to 75%, rendering the pipeline unreliable and dangerous. These findings underscore the critical importance of timely corrosion protection measures to mitigate the risk of pipeline failure over its operational lifespan.

The trends and the reliability of the risk assessment approach were confirmed by comparing the results with established failure probability models and stress analysis techniques. This confirmation emphasizes the importance of proactive maintenance and

**Wokocha Heanyichukwu, Nitonye Samson, Sidum Adumene and Morrison Inegiyemiema**



corrosion management strategies in ensuring pipeline safety and reliability.

### **3.7. Proposed Comprehensive Offshore Pipeline Integrity Management Framework**

The proposed comprehensive offshore pipeline integrity management framework addresses the integration of failure probability and stress load effects to effectively manage corrosion impacts on offshore pipelines, ensuring their long-term integrity and reliability. By adopting a probabilistic approach, the framework assesses the likelihood of pipeline failure based on corrosion rates, environmental conditions, and operational stress loads, facilitating targeted mitigation strategies. Key components include risk assessment and failure probability analysis using advanced modelling techniques, stress load evaluations of internal and external forces, and a proactive monitoring program for early detection of corrosion defects. Additionally, the framework outlines targeted mitigation measures, such as cathodic protection and corrosion-resistant coatings, along with a maintenance plan for continuous integrity management. This comprehensive approach enhances risk management, improves reliability and safety, and optimizes operational and lifecycle management.

### **4. CONCLUSION:**

The current study presents a comprehensive analysis of offshore pipelines' corrosion behavior and integrity management strategies. Several

models were used to ascertain the system behavior under defects and how the pipeline could be managed to mitigate failures. The research findings reveal

- The environmental corrosion influential factors, such as temperature, salinity, and dissolved oxygen, significantly influence corrosion rates, with higher temperatures correlating to increased corrosion,
- Corrosion rates rise significantly with water temperatures above 15°C but progress more slowly below this threshold with time.
- The empirical and exponential models show different trends in the corrosion rate profile for the period under consideration.
- A strong correlation between the increased corrosion defect length and decreased failure stress ratio. For instance, after 25 years of corrosion initiation without protection, the pipeline can handle only 20% of its original design stress, making it susceptible to failure.
- The evaluation of various corrosion mitigation techniques—such as cathodic protection, protective coatings, and inhibitors—indicates that a combination of these methods is most effective, providing practical guidance for operators.
- That corrosion depth profiles provide adequate information for predicting the pipeline's long-term degradation and maintenance timeline.

A structured integrity management framework was also developed, integrating failure

**Wokocha Heanyichukwu, Nitonye Samson, Sidum Adumene and Morrison Inegiyemiema**



probability analysis, stress load assessments, and targeted mitigation strategies. This framework serves as a comprehensive tool for offshore pipeline operators, facilitating proactive maintenance planning and ensuring the long-term reliability of their systems.

## REFERENCES

Abbas, M., & Shafiee, M. (2020). An overview of maintenance management strategies for corroded steel structures in extreme marine environments. *Marine Structures*, 71, 102718.

Adumene, S., Khan, F., Adedigba, S., Zendeheboudi, S., & Shiri, H. (2020). Dynamic risk analysis of marine and offshore systems suffering microbial-induced stochastic degradation. *Reliability Engineering & System Safety*, 207, 107478.

Axelsen, S. B., Knudsen, O.Ø., & Johnsen, R. (2010). Protective coatings offshore: Introducing a risk-based maintenance management system—Part 2: Framework establishment. *Corrosion*, 66(1), 1–10.

Bai, Q., & Bai, Y. (2014). *Force model and wave fatigue*. In *Subsea pipeline design, analysis, and installation* (pp. 365–384). Gulf Professional Publishing.

Bai, Y., & Bai, Q. (2014). *Corrosion and corroded pipelines*. In *Subsea pipeline integrity*

*and risk management* (pp. 3–25). Gulf Professional Publishing.

Bastos, I. N., Tavares, S. S. M., Dalard, F., & Nogueira, R. P. (2007). Effect of microstructure on corrosion behavior of super duplex stainless steel at critical environment conditions. *Scripta Materialia*, 57, 913–916.

Bhushan, B., & Luo, D. (2018). Nanomechanical and nanotribological characterization of marine organisms and biomimetics. In *Nanotribology and nano-mechanics* (pp. 1–43). Springer, Cham.

Bia, N., Shanhua, X., & Youde, W. (2019). Time-dependent reliability analysis of corroded steel beam. *KSCE Journal of Civil Engineering*, 24, 255–265.

Cao, X., Zhang, J., Xu, L., & Sun, Y. (2017). Corrosion behavior of pipeline steel in the presence of natural biofilms in a simulated marine environment. *Electrochimica Acta*, 236, 53–62.

Cheng, L., Chen, M., & Li, S. (2019). Corrosion detection of underwater pipelines using an adaptive T-scan technique. *Measurement Science and Technology*, 30(3), 035105.

Clover, D., Kinsella, B., Pejicic, B., & De Marco, R. (2005). The influence of microstructure

**Wokocha Heanyichukwu, Nitonye Samson, Sidum Adumene and Morrison Inegiyemiema**





- on the corrosion rate of various carbon steels. *Journal of Applied Electrochemistry*, 35, 139–149.
- David, E. U., Daniel, T., & Victor, E. O. (2023). Corrosion-based integrity analysis of offshore pipeline for hydrocarbon transportation. *Journal of Power and Energy Engineering*, 11(5), 1–10.
- David, V. S., & Ramana, M. P. (2010). A theoretical model for metal corrosion degradation. *International Journal of Corrosion*, Article ID 105034.
- DNV. (2010). *Cathodic protection design*. Recommended Practice RP, DNV Corporate Headquarters, Oslo, Norway.
- Evans, U. R. (2008). Perspectives on corrosion science and engineering. *Corrosion Science*, 50(2), 589–604.
- Guedes, C., Zayed, A., & Garbatov, Y. (2011). Effect of environmental factors on steel plate corrosion under marine immersion conditions. *Corrosion Engineering, Science and Technology*, 46, 524–541.
- Hameed, H., Bai, Y., & Ali, L. (2020). A risk-based inspection planning methodology for integrity management of subsea oil and gas pipelines. *Ships and Offshore Structures*, 1–13.
- <https://doi.org/10.1080/17445302.2020.1763405>
- Hwang, B., Kim, Y. M., Lee, S., Kim, N. J., & Ahn, S. S. (2005). Correlation of microstructure and fracture properties of API X70 pipeline steels. *Metallurgical and Materials Transactions A*, 36, 725–739.
- Johnson, A., & Smith, J. (2019). Effect of flow velocity on offshore pipeline corrosion rates: A case study in the Gulf of Mexico. *Corrosion Engineering*, 28(2), 89–105.
- Johnson, M. W., & Garcia, R. M. (2017). Offshore pipeline corrosion monitoring systems: Case studies and best practices. *Journal of Corrosion Science*, 45(5), 678–689.
- Katiyar, P. K., Behera, P. K., Misra, S., & Mondal, K. (2019a). Effect of microstructures on the corrosion behavior of reinforcing bars (rebar) embedded in concrete. *Metals and Materials International*, 25, 1209–1226.
- Katiyar, P. K., Misra, S., & Mondal, K. (2019b). Comparative corrosion behavior of five microstructures (pearlite, bainite, periodized, martensite, and tempered martensite) made from a high carbon steel. *Metallurgical and Materials Transactions A*, 50, 1489–1501.





- Khristenko, U., Constantinescu, A., Le, T. P., & Oden, J. T. (2019). A statistical framework for generating microstructures of two-phase random materials: Application to fatigue analysis. *Journal of the Mechanics and Physics of Solids*, 129, 95–109.
- Kiefner, J. F., & Vieth, P. H. (1990). Evaluating pipe: New method corrects criterion for evaluating corroded pipe. *Oil & Gas Journal*, 88(32), 56–59.
- Melchers, R. E. (2005). The effect of corrosion on the structural reliability of steel offshore structures. *Corrosion Science*, 47, 2391–2410.
- Nitonye, S., Nwaoha, T. C. & Ofonime, E. (2020) Use of *Vernonia Amygdalina* (VA) as a Corrosion Inhibitor on Subsea Transmission Pipeline. *FUW Trends in Science & Technology Journal*, April 2020: 5(1), 177 – 183. [www.ftstjournal.com](http://www.ftstjournal.com)
- Nitonye, S., Ofonime, E. & Ogbonnaya, E. A., (2018) Combating Corrosion in Transmission Pipelines in Marine Environment using *Vernonia Amygdalina* as Inhibitor. *Open Journal of Marine Science*, 8(4), 450-472. <https://doi.org/10.4236/ojms.2018.84025> <http://www.scirp.org/journal/ojms>
- Pohlman, S. L. (1987). General corrosion. In J. R. Davis *et al.* (Eds.), *Metals handbook* (9th ed., Vol. 13, pp. 9–22). ASM International.
- Qin, S., & Cui, W. (2003). Effect of corrosion models on the time-dependent reliability of steel plated elements. *Marine Structures*, 16, 15–34.
- Rezakhani, D. (2011). The effects of temperature, dissolved oxygen, and the velocity of seawater on the corrosion behavior of condenser alloys. *Anti-Corrosion Methods and Materials*, 58(2), 90–94.
- Sun, F., Li, X., & Cheng, X. (2018). Effects of carbon content and microstructure on corrosion property of new developed steels in acidic salt solutions. *Acta Metallurgica Sinica (English Letters)*, 27, 115–123.
- Wang, S., Lamborn, L., & Chen, W. (2021). Near-neutral pH corrosion and stress corrosion crack initiation of a mill-scaled pipeline steel under the combined effect of oxygen and paint primer. *Corrosion Science*, 187, 109511.
- Williams, R. S., & Brown, L. H. (2019). A comprehensive review of offshore pipeline corrosion factors. *Corrosion Review*, 32(2), 143–158.

# **Irish International Journal of Engineering and Scientific Studies**

I. Int. J. Eng. Sci. S.

Volume: 8; Issue: 01,

January-February, 2025

ISSN: 2853-4387

Impact Factor: 7.96

Advance Scholars Publication

Published by International Institute of Advance Scholars Development

<https://aspjournals.org/Journals/index.php/ijess>



- Xue, H. B., & Cheng, Y. F. (2011). Characterization of inclusions of X80 pipeline steel and its correlation with hydrogen-induced cracking. *Corrosion Science*, 53, 1201–1208.
- Zhang, Y., Zhu, W., & Dugstad, A. (2020). Predicting corrosion rate of offshore steel structures using artificial intelligence techniques. *Ocean Engineering*, 209, 107467.

**Wokocha Heanyichukwu, Nitonye Samson, Sidum Adumene and Morrison Inegiyemiema**